THE JOURNAL OF BIOLOGICAL CHEMISTRY VOL. 282, NO. 20, pp. 15271–15283, May 18, 2007

The Nucleoside Analog Sangivamycin Induces Apoptotic Cell Death in Breast Carcinoma MCF7/Adriamycin-resistant Cells via Protein Kinase Cδ and JNK Activation*[S]

Received for publication, February 15, 2007 Published, JBC Papers in Press, March 19, 2007, DOI 10.1074/jbc.M701362200

Sung A. Lee and Mira Jung[1]

From the Department of Radiation Medicine, Georgetown University Medical Center, Washington, D. C. 20057-1482

Sangivamycin has shown a potent antiproliferative activity against a variety of human cancers. However, little is known about the mechanism of action underlying its antitumor activity. Here we demonstrate that sangivamycin has differential antitumor effects in drug-sensitive MCF7/wild type (WT) cells, causing growth arrest, and in multidrug-resistant MCF7/adriamycin-resistant (ADR) human breast carcinoma cells, causing massive apoptotic cell death. Comparisons between the effects of sangivamycin on these two cell lines allowed us to identify the mechanism underlying the apoptotic antitumor effect. Fluorescence-activated cell sorter analysis indicated that sangivamycin induced cell cycle arrest in the G_2/M phase in MCF7/ADR cells. A marked induction of c-Jun expression as well as phosphorylation of c-Jun and JNK was observed after sangivamycin treatment of MCF7/ADR cells but not MCF7/WT cells. Sangivamycin also induced cleavage of lamin A and poly(ADP-ribose) polymerase (PARP) in MCF7/ADR cells, probably via activation of caspase-6, -7, and -9. Pretreatment with a caspase-9-specific inhibitor or pan-caspase inhibitor abolished sangivamycin-induced cleavage of lamin A and PARP but not sangivamycin induction of c-Jun expression and phosphorylation. Pretreatment of MCF7/ADR cells with SP600125, a specific inhibitor of JNK, or with rottlerin, a specific inhibitor of protein kinase Cδ (PKCδ), significantly reduced the sangivamycin-induced apoptosis and almost completely abolished sangivamycin-induced phosphorylation of c-Jun and cleavage of lamin A and PARP. Transfection of MCF7/ADR cells with PKCδ small interfering RNAs or PKCδ antibody or rottlerin pretreatment significantly suppressed the phosphorylation of JNK. Taken together, our data suggest that sangivamycin induces mitochondria-mediated apoptotic cell death of MCF7/ADR cells via activation of JNK in a protein kinase Cδ-dependent manner.

4-Amino-5-carboxamide-7-(D-ribofuranosyl)pyrrolo[2,3-*d*]pyrimidine (sangivamycin),[2] a naturally occurring deazapurine nucleoside analog antibiotic originally isolated from *Streptomyces rimosus*, was found to have antiviral activity (1–2). It has potent cytotoxic activity in transformed and tumorigenic cells *in vitro* (3–5) and a significant antitumor activity without serious toxicity *in vivo* (6, 7). Sangivamycin and its derivatives have been evaluated as potential anticancer agents against a variety of human cancers, including mammary carcinoma and leukemia (8–13). Its ability to function as a protein kinase inhibitor has been demonstrated; it is a potent inhibitor of both protein kinase C (K_i of 10 μM) and rhodopsin kinase (K_i of 180 nM). At higher concentrations sangivamycin also inhibits protein kinase A (IC_{50}: 50 μM) and β-adrenergic receptor kinase (K_i of 67 μM) (14–16). Its inhibitory activity against partially purified nuclear protein kinases has also been reported; sangivamycin inhibited phosphorylation of histone H1 by partially purified nuclear protein kinase I (K_i of 200 μM) and phosphorylation of casein by nuclear protein kinase II (K_i of 100 μM) (17). Inhibition of cell cycle progression at the G_2 phase in tsFT210 cells, a temperature-sensitive mutant of the mouse mammary carcinoma cell line FM3A, by sangivamycin (10 μM), has also been reported (18). Recently, a synthetic non-nucleoside analog of sangivamycin was shown to induce apoptosis in human leukemia cells via caspase-dependent Bid cleavage and release of cytochrome *c* from mitochondria (19). However, the mechanism of action underlying the antitumor activity of sangivamycin remains unknown.

Apoptosis, programmed cell death, plays an essential role in normal development and tissue homeostasis. Disruption of regulated apoptotic processes leads to various physiological abnormalities including cancer, autoimmune diseases, and neurodegenerative disorders (20–24). Bcl-2 family member proteins and caspases have been associated with the apoptotic processes (25–27). The Bcl-2 family can be classified into two subsets, anti-apoptotic proteins such as Bcl-2, Bcl-x/L, and Mcl-1, and proapoptotic proteins such as Bax, Bak, Bid, and Bcl-x/S. Each subset can form homodimers as well as heterodimers with members of the other subset, resulting in the neutralization of opposing activities. Actually, the ratio between these two subsets helps determine in part the susceptibility of cells to death promoting signals (28, 29). Activation of proapoptotic Bcl-2 family members leads to the release of cytochrome *c* and other apoptogenic factors, such as Smac, from the mitochondrial

* This work was supported by NCI, National Institutes of Health Grants P02 CA74175. The costs of publication of this article were defrayed in part by the payment of page charges. This article must therefore be hereby marked "*advertisement*" in accordance with 18 U.S.C. Section 1734 solely to indicate this fact.

[S] The on-line version of this article (available at http://www.jbc.org) contains supplemental Figs. 1–3.

[1] To whom correspondence should be addressed. Tel.: 202-687-8352; Fax: 202-687-2221; E-mail: jungm@georgetown.edu.

[2] The abbreviations used are: sangivamycin, 4-amino-5-carboxamide-7-(D-ribofuranosyl)pyrrolo[2,3-*d*]pyrimidine; PKC, protein kinase C; JNK, c-Jun NH_2-terminal kinase; PARP, poly(ADP-ribose) polymerase; ADR, adriamycin-resistant; CHAPS, 3-[(3-cholamidopropyl)dimethylammonio]propane sulfonate; MTT, 3-(4,5-dimethylthiazol-2-yl)-2,5-diphenyltetrazolium bromide; siRNA, short interference RNA; WT, wild type.

intermembrane space to the cytoplasm, resulting in activation of caspase cascades (caspase-9 and -3). Induction of caspase activities can also occur by interfering with caspase inhibitors (28–30).

The apoptotic cell death triggered by many chemotherapeutic agents commonly involves stress-transducing kinases, culminating at the mitochondria. Involvement of protein kinase C in the process of apoptosis has been demonstrated (31, 32). Protein kinase Cδ is a proapoptotic kinase that has been associated with cellular responses to DNA damage and apoptotic cell death (33–35). Increasing amounts of evidence suggest that proteolytic cleavage of PKCδ by downstream effector caspases to a 40-kDa active kinase is required for the proapoptotic activity of PKCδ (36–38).

Activation of the stress-activated protein kinase pathway has been associated with the apoptotic response induced by some chemotherapeutic agents and other DNA damaging agents (39–42). Activation of c-Jun NH_2-terminal kinase (JNK) isoforms and the phosphorylation of transcription factors like c-Jun and ATF2 as well as pro- and anti-apoptotic Bcl-2 family members such as Bim, Bcl-2, and Bcl-x/L have been suggested to be important in the regulation of apoptosis (43–45).

In the present study we examined the molecular consequences of treating two human breast carcinoma cell lines, drug-sensitive MCF7/WT and multidrug-resistant MCF7/ADR with sangivamycin. These studies focus on understanding why sangivamycin induces apoptosis only in the drug-resistant MCF7/ADR cell line.

EXPERIMENTAL PROCEDURES

Materials—Pan-caspase inhibitor (benzyloxycarbonyl-VAD-fluoromethyl ketone) and caspase 9-specific inhibitor (benzyloxycarbonyl-LEHD-fluoromethyl ketone) were purchased from Calbiochem. Rottlerin and SP600125 were from BioMol. Antibodies to 89-kDa cleaved poly(ADP-ribose) polymerase (PARP), lamin A, cleaved caspase 6, caspase-7 and -9, and c-Jun phosphorylated on Ser^{63} or on Ser^{73} and JNK phosphorylated on Thr^{183} and Tyr^{185} were from Cell Signaling Technology. Antibody to c-Jun was from Transduction Laboratories. Antibodies to Bcl-2, Bcl-x/L, Bax, and PKCδ were purchased from Santa Cruz. Antibodies to p21 and Bcl-x/S were from Oncogene Sciences. PKCδ ON-TARGETplus siRNA, ON-TARGETplus siCONTROL Non-targeting pool, c-Jun siRNA SMARTpool, Non-targeting siCONTROLpool, and DharmaFECT 1 transfection reagent were purchased from Dharmacon. Chariot protein transfection reagent was from Active Motif. Alexa Fluor 488- and Alexa Fluor 594-conjugated secondary antibodies and MitoTracker red were purchased from Molecular Probes. Sangivamycin was obtained from Natural Products Branch, Division of Cancer Treatment, NCI, National Institutes of Health.

Cell Culture—MCF7 human breast cancer cell lines (drug-sensitive MCF7/WT cells and multidrug-resistant MCF7/ADR cells) were cultured in a complete medium; RPMI 1640 medium supplemented with 10% fetal bovine serum, 2 mM L-glutamine, penicillin (100 units/ml), and streptomycin (100 μg/ml) at 37 °C under a humidified atmosphere of 5% CO_2 in air. MCF7/ADR cells were routinely monitored for their resistance to adriamycin. To maintain a highly drug-resistant cell population, the multidrug-resistant MCF7/ADR cells were periodically reselected by growing them in the presence of increasing concentrations of adriamycin (7–10 μM) for ~2-month periods of time as described previously (46).

Cytotoxicity and Cell Cycle Analyses—For the sangivamycin dose-response experiment, MCF7 cells were seeded in 24-well plates (in triplicate) at a density of ~20,000 cells/well in a complete medium. After 24 h the medium was replaced with 1-ml aliquots of RPMI 1640 medium supplemented with 2 mM L-glutamine, penicillin (100 units/ml), streptomycin (100 μg/ml), 10% heat-inactivated fetal bovine serum, and various concentrations of sangivamycin. After 72 h of incubation at 37 °C, 100 μl of MTT (5 mg/ml in Dulbecco's phosphate-buffered saline) was added to each well, and incubation was continued for another hour, and then the formazan precipitate was dissolved in 1 ml of Me_2SO. The relative numbers of viable cells were estimated from the changes in absorbance at 590 nm (46). To determine the long-term cytotoxicity of sangivamycin, MCF7 cells were seeded in 6-well plates at a density of 7000 cells/well for MCF7/WT and 9000 cells/well for MCF7/ADR cells in a complete medium. After 24 h, cells were treated with or without 0.3 μM sangivamycin in RPMI 1640 medium supplemented with 2 mM L-glutamine, penicillin (100 units/ml), streptomycin (100 μg/ml), and 10% heat-inactivated fetal bovine serum for 6 days. Viable cells remaining in each well were trypsinized and counted using Coulter cell counter. For cell cycle analysis, the cells were harvested at the indicated time points and washed twice with cold phosphate-buffered saline. Cells ($1–2 \times 10^6$) were resuspended in 0.5 ml of ice-cold phosphate-buffered saline, and single cell suspension was verified microscopically. The cell suspension was gradually mixed with ice-cold absolute ethanol to the final volume of 2.0 ml and put on ice at least for 20 min before staining with propidium iodide. The cell cycle distributions were measured in a fluorescence-activated cell sorter (FACSort) from BD Biosciences. DNA content was quantified using ModFit LT 3.0 software (Verity Software House, Inc.).

Transient Transfection of MCF7/ADR Cells with c-Jun siRNA or PKCδ siRNA—MCF7/ADR cells were seeded in 35-mm dishes or in a 4-well chamber slide at a density of ~150,000 cells/dish or 25,000 cells/well, respectively, in complete medium. After 24 h cells were transfected with 100 nM siRNA or siCONTROL using DharmaFECT 1 transfection reagent as suggested by the manufacturer (Dharmacon). At 48 h post-transfection, cell culture medium was supplemented with a final concentration of 0.3 μM sangivamycin or vehicle without removing the medium containing siRNA and the transfection reagent, and cells were continuously incubated for an additional 48 h until they were harvested or fixed for further analysis.

Delivery of PKCδ Antibody into Live MCF7/ADR Cells Using Chariot—MCF7/ADR cells were seeded in 4-well chamber slides at a density of ~30,000 cells/well in the complete medium. After 24 h, cells were transfected with PKCδ COOH terminus antibody using Chariot protein transfection reagent as instructed by the manufacturer (Active

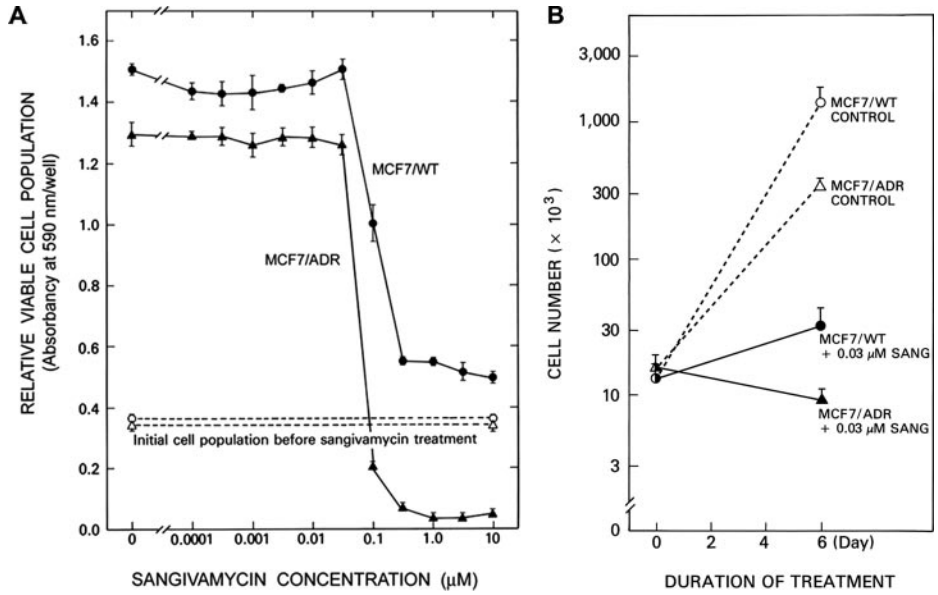

FIGURE 1. **Effects of various concentrations of sangivamycin on cell growth of drug-sensitive human breast carcinoma MCF7/WT cells and multidrug-resistant MCF7/ADR cells.** *A*, dose response of sangivamycin effects on cell viability. The relative viability of cells incubated with various concentrations of sangivamycin for 72 h was determined by MTT colorimetric assay. The results shown are representative plots of three or more independent experiments, each done in triplicate. *B*, effects of suboptimal concentrations (30 nM) of sangivamycin on cell growth upon prolonged incubation for six days. Cytotoxicity was determined by counting viable cells after treatment as described under "Experimental Procedures."

Motif). At 3 h post-transfection, cell culture medium was supplemented with a final concentration of 0.3 μM sangivamycin or vehicle without removing the medium containing anti-PKCδ and Chariot, and cells were continuously incubated for an additional 48 h until they were fixed for immunofluorescent microscopic analysis.

Immunoblot Analysis—Cells were washed three times with ice-cold phosphate-buffered saline, harvested by scraping from the culture dishes into ice-cold equilibration buffer containing 20 mM Tris-HCl (pH 7.5), 2 mM EDTA, 2 mM EGTA, and protease inhibitors (47) and collected by centrifugation at 800 × *g* for 5 min at 4 °C. Cell pellets were solubilized with 1% (w/v) CHAPS in equilibrium buffer on ice for 1 h. The total cell extract was then isolated by centrifugation at 50,000 × *g* for 30 min at 4 °C. Protein concentrations were determined with the Bradford assay (48) with bovine serum albumin as a standard. Equal amounts of proteins were denatured by boiling for 5 min in SDS sample buffer and subjected to SDS-polyacrylamide gel electrophoresis. The separated proteins were transferred to a polyvinylidene difluoride membrane, and nonspecific IgG binding sites were blocked by incubation with 5% nonfat dry milk for 1 h at room temperature. The membrane was then incubated overnight at 4 °C with primary antibodies. Immune complexes were detected by enhanced chemiluminescence (Amersham Biosciences).

Confocal Immunofluorescent Microscopy—Cells were fixed in 4% paraformaldehyde, permeabilized with 0.1% Triton X-100, and blocked with 5% bovine serum albumin and 10% normal goat serum in phosphate-buffered saline. Primary antibody incubation was carried out overnight at 4 °C, and Alexa Fluor-conjugated-secondary antibody incubation was carried out for 1 h at room temperature. Immunofluorescence was detected and analyzed using an Olympus Fluoview FV300 confocal laser scanning biological microscope system and software (Olympus America). All experiments were repeated more than three times, and the representative results were presented.

RESULTS

Differential Effects of Sangivamycin on MCF7/WT and MCF7/ADR Cell Growth—To identify biological activities of sangivamycin relevant to its antitumor activity toward human breast carcinoma cells, we first compared the chemosensitivity of drug-sensitive human breast carcinoma MCF7/WT cells and multidrug-resistant MCF7/ADR cells to sangivamycin by examining the cell growth rate and morphological changes. Sangivamycin exhibited differential cytotoxicity toward MCF7/WT cells and MCF7/ADR cells (Fig. 1*A*). When MCF7/ADR cells were treated with 0.1 μM or higher concentrations of sangivamycin for 72 h, the number of viable cells was reduced to levels below that measured before the sangivamycin treatment, implying a cytocidal effect toward MCF7/ADR cells. In contrast, the numbers of viable MCF7/WT cells remaining after identical treatments with sangivamycin were slightly higher than the initial cell population, suggesting a cytostatic effect toward MCF7/WT cells. Similar results were observed when cells were treated with sangivamycin for 1 h followed by continued incubation in the absence of sangivamycin for 72 h, except that the dose-response curves were shifted to the right by one log scale, indicating irreversible cytocidal or cytostatic effects of sangivamycin in these cells (data not shown). A longer treatment (6 days) of these two cell lines with a lower concentration (30 nM) of sangivamycin resulted in similar responses (Fig. 1*B*). A similar pattern of cytocidal effect was also observed in another set of independently established drug-resistant MCF7 cell lines, MCF7/W0.3 and MCF7/W10 (46).

For the morphological study, a single pharmacological dose of sangivamycin was used, 0.3 μM, a concentration that showed almost maximal cytocidal (for MCF7/ADR) or cytostatic (for MCF7/WT) effects (Fig. 2*A*). Floating MCF7/ADR cells were observed within 24 h of sangivamycin addition, and most of the MCF7/ADR cells were floating by 72 h. The trypan blue dye exclusion test revealed that the majority of the floating MCF7/ADR cells (95% at 72 h) had intact plasma membranes (data not shown). In contrast, no significant number of floating MCF7/WT cells was observed within 72 h, although growth inhibition was apparent by 48 h (Fig. 2*A*). When cells were further incubated for 7 days without replenishment of sangivamycin after the initial treatment, a slow recovery of cell proliferation was observed in MCF7/WT cells, suggesting a reversi-

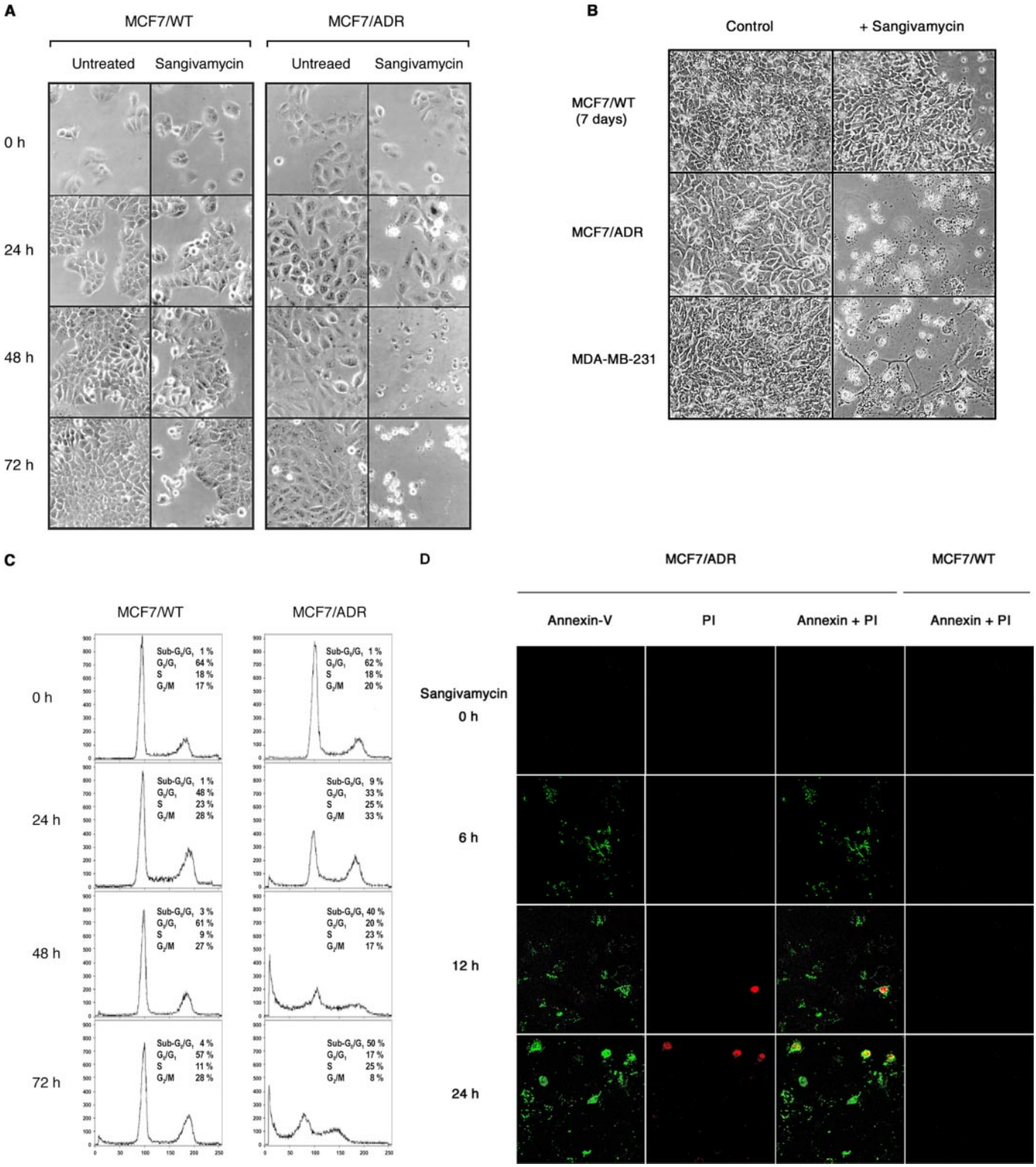

FIGURE 2. **Differential cytotoxicity of sangivamycin; cytocidal effect in MCF7/ADR cells and cytostatic effects in MCF7/WT cells.** *A*, chemosensitivity to sangivamycin was visually evaluated by monitoring the relative amounts of adherent cells after incubating with 0.3 μM sangivamycin for the indicated period of times using an Olympus Vanox microscopy. *B*, reversible cytostatic effect in drug-sensitive MCF7/WT cells and irreversible cytocidal effect in multidrug-resistant MCF7/ADR and MDA-MB-231 cells. Chemosensitivity to sangivamycin was visually evaluated by using an Olympus Vanox microscopy after incubating cells with 0.3 μM sangivamycin for 7 days. *C*, effects of sangivamycin on cell cycle progression and apoptosis. Cells were incubated with 0.3 μM sangivamycin for the indicated period of times, and their DNA contents were analyzed by propidium iodide (*PI*) fluorescence flow cytometry. Cells in the sub-G_0/G_1 region represent apoptotic cells. *D*, early stage apoptosis assay. Binding of fluorescein-conjugated annexin-V to phosphatidylserine translocated from the inner to the outer surface of plasma membrane in cells going through early stage apoptosis was visualized by using a confocal fluorescent microscopy (*green*). Cells with ruptured plasma membrane in the process of cell death were visualized by binding of propidium iodide to cellular nucleic acids (*red*).

ble cytostatic effect. However, a massive cell death was observed in MCF7/ADR cells as well as another multidrug-resistant metastatic breast cancer cell line, MDA-MB-231 (Fig. 2*B*), implicating an irreversible cytocidal effect of sangivamycin in these cells.

Sangivamycin-induced Inhibition of Cell Cycle Progression and Apoptotic Cell Death in MCF7/ADR Cells—To determine if the cell growth arrest by sangivamycin is associated with the stages of cell cycle, the cell cycle distribution was measured by fluorescence-activated cell sorter analysis. In MCF7/ADR cells the relative population size of cells in the G_0/G_1 phase continuously decreased over the 72-h period, whereas the relative S-phase population size was not affected significantly, and the G_2/M phase cell population initially increased by 24 h and decreased thereafter. Concomitantly, a continuous increase in the sub-G_1 cell population was observed with a marked increase after 24 h and sustained over 72 h; more than 50% of the cell population contained hypodiploid DNA content (sub-G_1 peak), a hallmark of apoptosis (Fig. 2*C*). These results suggest that sangivamycin induces a cell cycle arrest at G_2/M phase within 24 h, which is subsequently followed by a massive cell death in MCF7/ADR cells.

In contrast, MCF7/WT cells behaved differently in all subphases of cell cycle in response to sangivamycin; although there was an initial relative decrease in the G_0/G_1 population by 24 h, it returned to the original level by 48 h, the G_2/M-phase population increased by 24 h but stayed at that level, and the S-phase population was slightly increased by 24 h and then decreased significantly between 24–48 h. Furthermore, no evidence for a significant increase in DNA fragmentation was observed in MCF7/WT cells upon exposure of cells to sangivamycin, with only 4% of the population containing a hypodiploid DNA content at 72 h. These results suggest that cell cycle progression of MCF7/WT cells is also arrested at G_2/M phase within 24 h, but instead of massive cell death by 48 h, there is a second cell cycle arrest at the G_1 phase.

Apoptotic cell death observed in MCF7/ADR cells but not in MCF7/WT cells upon treatment with sangivamycin was further confirmed by determining annexin V binding to phosphatidylserine translocated from the inner to the outer membrane surface of the plasma membrane, a hallmark of early stage of apoptosis (Fig. 2*D*). In MCF7/ADR cells, annexin V binding was observed as early as 6 h after sangivamycin treatment, whereas binding of propidium iodide, a cell-impermeant dye, to the nucleic acids in the cell was observed after 12 h only in a minor fraction of annexin V-bound cells, implying cell death at the late stage of apoptosis. In MCF7/WT cells, in contrast, neither annexin V binding nor propidium iodide staining was observed even after 24 h of treatment with sangivamycin.

Because p53 plays a pivotal role in regulating a G_1 phase checkpoint and is required for G_2/M arrest (49), the effect of sangivamycin on p53 accumulation was determined (Fig. 3). MCF7/WT cells express a wild type p53, whereas MCF7/ADR cells express an inactive mutant p53 (a 21-bp deletion at the splicing acceptor site of exon 5, resulting in a slightly smaller size of p53 protein) (50–52). The basal level of p53 was significantly higher in MCF7/ADR cells, which gradually decreased to undetectable levels by 72 h after sangivamycin treatment. In

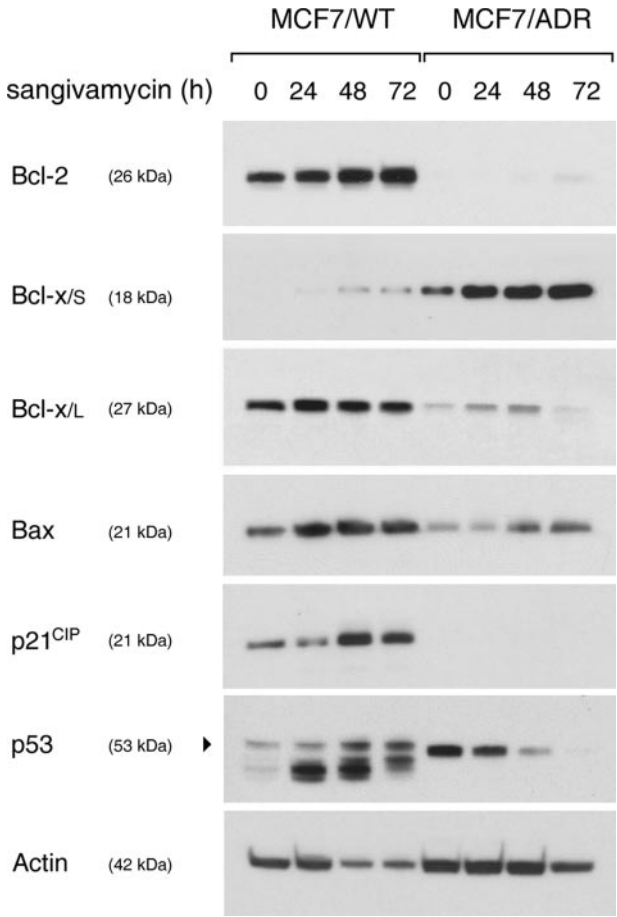

FIGURE 3. **Time course of the effects of sangivamycin on the accumulation of Bcl-2 family member proteins and p21^{CIP} in MCF7/WT and MCF7/ADR cells.** Cells were incubated with 0.3 μM sangivamycin for the indicated times. Total cell extracts were prepared and subjected to immunoblot analysis. Actin was used as a loading control.

contrast, sangivamycin treatment of MCF7/WT cells caused wild type full-length p53 to accumulate gradually, which was accompanied by a more rapid accumulation of 40–50-kDa proteins, presumably proteolytic cleavage products of p53 as speculated from their cross-immunoreactivity to the p53 antibody. Concomitantly, a substantial amount of p21^{CIP}, a cyclin-dependent kinase inhibitor, was present in MCF7/WT cells, which further increased by 48 h upon exposure to sangivamycin and then remained at the elevated level in MCF7/WT cells but not in MCF7/ADR cells.

Effects of Sangivamycin on the Relative Level of Various Proteins Involved in Apoptosis—To identify possible molecular mechanisms underlying the apoptotic cell death of MCF7/ADR cells but not MCF7/WT cells upon exposure to sangivamycin, we first investigated the effect of sangivamycin treatment on the relative amounts of some proteins known to be involved in various apoptotic events (Fig. 3). Surprisingly, profound differences were seen even in the untreated cells. The amount of two anti-apoptotic proteins, Bcl-2 and Bcl-x/L, was substantially higher in untreated MCF7/WT cells than in untreated MCF7/ADR cells. In contrast, the amount of proapoptotic protein Bcl-x/S was substantially higher in the untreated MCF7/ADR cells than in untreated MCF7/WT cells. Sangivamycin exposure increased these basal levels in both cell types except for Bcl-2 in

MCF7/ADR cells, which remained undetectable. Thus, MCF7/ADR cells contain substantially higher levels of a proapoptotic protein, Bcl-x/s, and substantially lower levels of two anti-apoptotic proteins, Bcl-2 and Bcl-x/l, compared with MCF7/WT cells both before and after sangivamycin treatment. However, a different pattern was observed with another proapoptotic protein, Bax, which was present at higher levels in untreated MCF7/WT cells than in untreated MCF7/ADR cells. Although the relative -fold induction of Bax in MCF/ADR cells after sangivamycin treatment appeared to be greater than in MCF7/WT cells, the total accumulation after 72 h in MCF7/ADR cells was merely more or less at the uninduced level in MCF7/WT cells.

Effects of Sangivamycin on Activation of Caspases and Cleavage of Their Substrate Proteins—Activation of caspases during apoptosis results in the cleavage of various cellular substrates including lamins and PARP (53–55). To determine if sangivamycin activates caspases in MCF7/WT and MCF7/ADR cells, we examined cleavage of lamin A and PARP after treatment with 0.3 μM sangivamycin (Fig. 4*A*). Lamin A is a 70-kDa nuclear membrane protein and is cleaved to a 40–45-kDa fragment and a 28-kDa fragment during apoptosis (53, 56), resulting in nuclear disregulation and cell death (57, 58). Cleavage of lamin A was detected using antibody specifically recognizing a 28-kDa fragment. MCF7/ADR cells have a higher basal level of lamin A than MCF7/WT cells. Upon exposure of MCF7/ADR cells to sangivamycin, a vast amount of cleavage of lamin A to a 28-kDa fragment was detected within 48 h. Lamin A cleavage was not detectable in MCF7/WT cells after exposure to sangivamycin.

Another caspase substrate, nuclear protein PARP, which is involved in DNA repair and is important for maintaining cell viability (59), is cleaved to a 89-kDa fragment and a 24-kDa fragment during apoptosis. Cleavage of PARP facilitates cellular disassembly and serves as a marker for identifying cells undergoing apoptosis (60). After sangivamycin exposure, cleavage of PARP was detected using an antibody recognizing the 89-kDa fragment but not full-length 116-kDa PARP. The 89-kDa PARP fragment was observed only in MCF7/ADR cells, where a profound amount was accumulated by 48 h after sangivamycin treatment and further accumulated by 72 h as a broad diffuse band tending toward lower mobility, implicating a further post-translational modification such as a poly(ADP)-ribosylated or chromatin-associated form of the 89-kDa PARP fragment after 48 h. A similar result was also observed in two other multidrug-resistant metastatic breast cancer cell lines, MDA-MB-468 (supplemental Fig. 1) and MDA-MB-231 cells, but not in a non-malignant mammary epithelial breast cell line, MCF10A (data not shown). These data suggest that apoptotic cell death might be a prevalent mode of action of sangivamycin in a broad range of multidrug-resistant aggressive breast cancer cell lines.

Caspases exist as inactive pro-enzymes that undergo proteolytic processing to form activated enzymes, which play pivotal roles in the execution of apoptosis. Activation of caspase-6, -7, and -9 were measured by assessing the cleaved forms of these enzymes (Fig. 4*B*). As expected from the lamin A and PARP cleavage results (Fig. 4*A*), MCF7/ADR, but not MCF7/WT cells, contained the cleaved forms of caspase-6, -7, and -9 upon sangivamycin exposure. To further confirm that the sangivamycin-induced apoptosis of MCF7/ADR cells was caspase-dependent, MCF7/ADR cells were pretreated with a caspase-9-specific inhibitor or a pan-caspase inhibitor before sangivamycin treatment, and cleavage of lamin A and PARP was subsequently examined (Fig. 4*C*). Pretreatment with the pan-specific inhibitor completely abolished the cleavage of both lamin A and PARP, and the pharmacological inhibitor specific for caspase-9 also showed a significant inhibition of the cleavage of lamin A and PARP. These results strongly suggest that caspase-9 is cleaved and activated upon exposure of MCF7/ADR cells to sangivamycin and that the subsequent activation of the downstream caspase cascades accounts, at least in part, for the observed selective apoptotic cell death of MCF7/ADR cells.

Protein Kinase Cδ-dependent Activation of JNK in Sangivamycin-treated MCF7/ADR Cells—It has been demonstrated that sustained activation of c-Jun is sufficient to trigger apoptosis, which involves the activation of caspase signaling (61). The possible involvement of c-Jun/JNK pathway in sangivamycin-induced apoptosis of MCF7/ADR cells was investigated. JNK activation is mediated by phosphorylation of the threonine 183 and tyrosine 185 residues in the conserved TPY tripeptide motif in the kinase domain (42). Therefore, dually phosphorylated JNK at threonine 183 and tyrosine 185 was determined after 48-h treatment of cells with sangivamycin (Fig. 5*A*). A profound induction of p54 isoform as well as substantial induction of p46 isoform of phosphorylated JNK was observed in MCF7/ADR cells but not in MCF7/WT cells. Concomitantly, a time-dependent induction of c-Jun expression and sustained phosphorylation of c-Jun at serine 73 (Fig. 5*B*) and serine 63 (Fig. 5*C*) were observed in MCF7/ADR. Sangivamycin, however, did not induce c-Jun expression or phosphorylation in MCF7/WT cells where growth arrest occurs but not apoptosis.

Next, to determine if induction of c-Jun expression and phosphorylation by sangivamycin in MCF7/ADR cells was dependent on PKCδ activity, we used three experimental approaches. First, pretreatment of MCF7/ADR cells with 20 μM rottlerin, a specific inhibitor of PKCδ, for 1 h significantly reduced the induction of c-Jun expression and phosphorylation and suppressed the caspase-9 activation, cleavage of lamin A and PARP by sangivamycin (Fig. 5*C*). Secondly, transfection of MCF7/ADR cells with PKCδ antibody raised against the catalytic domain using protein transfection reagent, Chariot, significantly inhibited sangivamycin-induced JNK phosphorylation in MCF7/ADR cells (Fig. 5*D*). Statistical analysis of the immunofluorescence shown in Fig. *5D* using Fluoview FV300 confocal laser microscope system software revealed that immunofluorescence of the activated form of phosphorylated JNK was increased by 18–21-fold in sangivamycin-treated MCF7/ADR cells as compared with the untreated control cells (supplemental Fig. *2*). Rottlerin pretreatment or transfection of MCF7/ADR cells with PKCδ antibody using Chariot reduced the sangivamycin-induced immunofluorescence by 12 or 10-fold, respectively (data not shown). Lastly, the relationship between PKCδ expression and phosphorylation of JNK was examined in MCF7/ADR cells treated with sangivamycin for 48 h after transfection with PKCδ siRNAs (Fig. 5*E*). In a major-

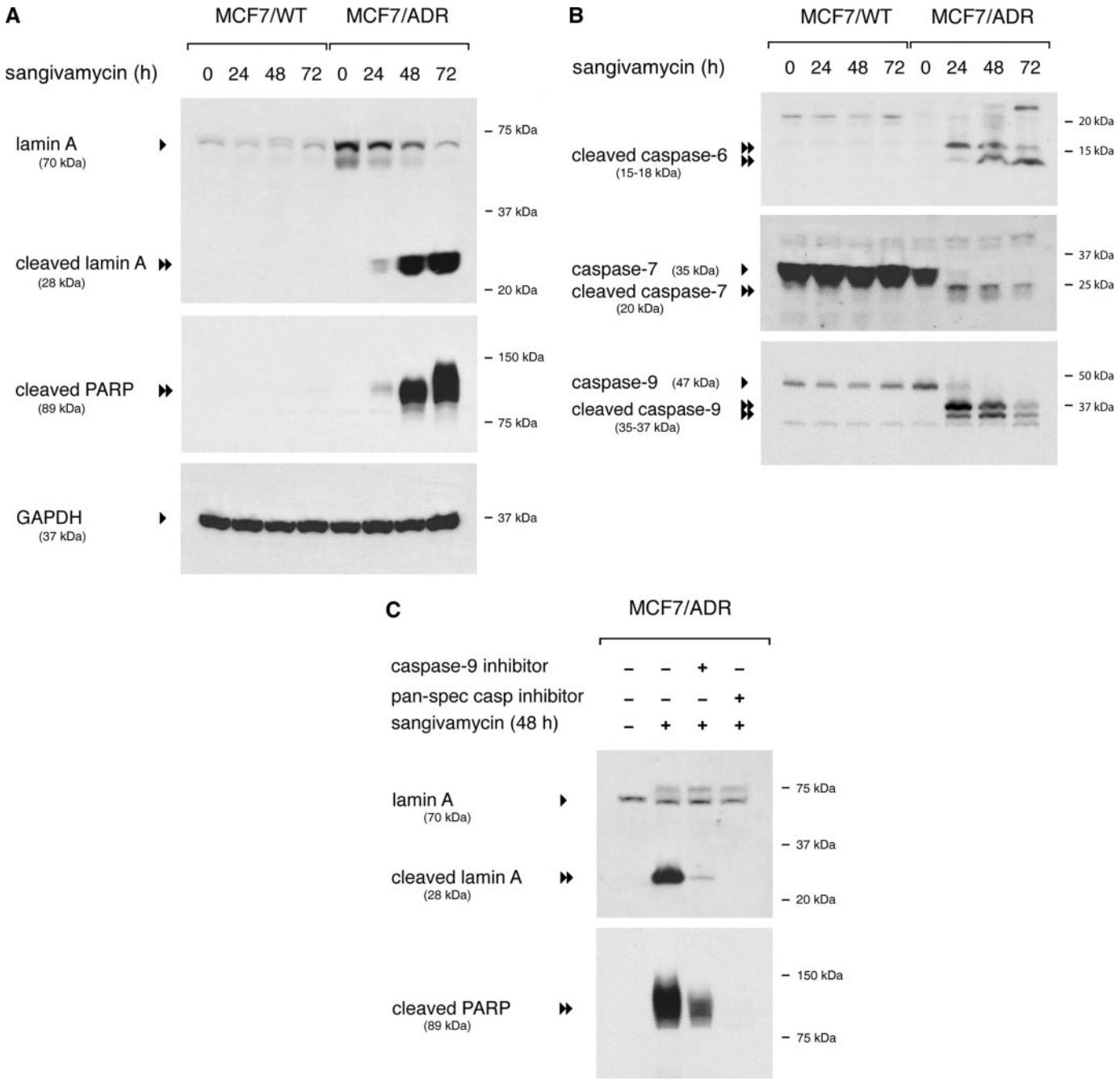

FIGURE 4. **Activation of caspases in sangivamycin-treated MCF7/ADR cells.** Total cell extracts were prepared from cells incubated with 0.3 μM sangivamycin for the indicated times and subjected to immunoblot analysis. glyceraldehyde-3-phosphate dehydrogenase (*GAPDH*) was served as a loading control. *A*, cleavage of lamin A and PARP in sangivamycin-treated MCF7/ADR cells. Cleavage products were detected using antibodies specific for the full-length and 28-kDa fragment of lamin A and for the 89-kDa cleaved fragment of PARP. *B*, activation of caspase-6, -7, and -9 in sangivamycin-treated MCF7/ADR cells. Activation was assessed by detection of the cleaved, active forms of these caspases. *C*, involvement of caspase-9 activation in sangivamycin-induced apoptosis of MCF7/ADR cells. Cells were pretreated for 1 h with 25 μM caspase-9 inhibitor or 50 μM pan-specific caspase inhibitor and then further incubated in the presence of 0.3 μM sangivamycin for an additional 48 h. Cleavage of lamin A and PARP was subsequently determined by immunoblot analysis of total cell extracts.

ity of cells in which the PKCδ expression was knock down by PKCδ siRNA, sangivamycin treatment did not induce phosphorylation of JNK; only a minor fraction of cells where PKCδ expression was not abolished exhibited phosphorylation of JNK upon exposure to sangivamycin. Taken together, these data indicate that sangivamycin treatment of MCF7/ADR cells induces PKCδ-dependent activation of JNK, resulting in the induction of c-Jun expression and phosphorylation.

Activation of Caspases in Sangivamycin-treated MCF7/ADR Cells Is Dependent on Activation of JNKs—Phosphorylation of c-Jun at serine 63 and serine 73 is mediated by JNK in response to various stimuli (62–66). Emerging evidence supports a role for JNK in stress-induced mitochondrial apoptotic pathways in a variety of cell systems (67–71). To confirm that the profound induction of c-Jun observed in sangivamycin-treated MCF7/ADR cells was mediated through activation of JNK, c-Jun

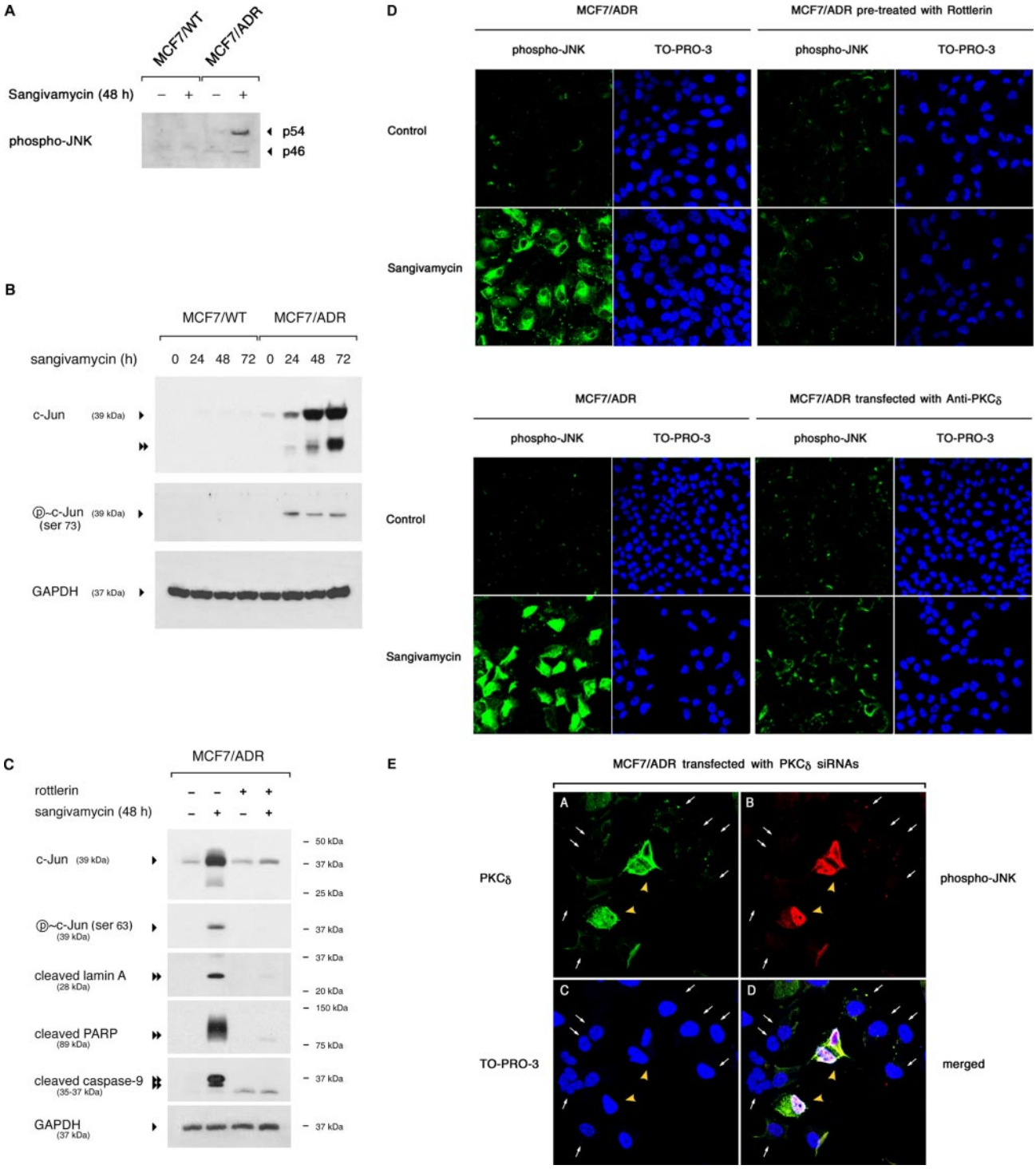

FIGURE 5. **PKCδ-dependent activation of JNK and apoptosis in sangivamycin-treated MCF7/ADR cells.** *A*, activation of JNK in sangivamycin-treated MCF7/ADR cells. Cells were incubated with 0.3 μM sangivamycin for 48 h and subjected to immunoblot analysis using antibody specific for the dually phosphorylated JNK (Thr^{183} and Tyr^{185}). *B*, induction of c-Jun expression and phosphorylation (*p-*) in sangivamycin-treated MCF7/ADR cells. Cells were incubated with 0.3 μM sangivamycin for the indicated times. Total c-Jun present in cells was detected by using c-Jun antibody recognizing both nonphosphorylated and phosphorylated form of c-Jun. Phosphorylation of c-Jun was analyzed using antibody specific for c-Jun phosphorylated at serine 73. *C*, PKCδ-dependent apoptosis and activation of c-Jun in sangivamycin-treated MCF7/ADR cells. Cells were pretreated with 20 μM rottlerin for 1 h before treatment of cells with 0.3 μM sangivamycin for 48 h and subjected to immunoblot analysis. Glyceraldehyde-3-phosphate dehydrogenase (*GAPDH*) was used as a loading control. *D*, inhibition of sangivamycin-induced activation of JNK by suppression of PKCδ activity. After pretreatment of MCF7/ADR cells with rottlerin or transfection with the catalytic domain anti-PKCδ using Chariot protein transfection reagent, cells were further incubated with 0.3 μM sangivamycin for 48 h and subjected to immunocytochemical analysis. Immunofluorescence of phosphorylated JNK (*green*) was detected using an Olympus Fluoview FV300 confocal laser microscope system. The nucleus was stained using nucleic acid-binding fluorescent dye, TO-PRO-3 (*blue*). *E*, inhibition of sangivamycin-induced activation of JNK by suppression of PKCδ expression. MCF7/ADR cells which had been transfected with PKCδ siRNA for 72 h were treated with 0.3 μM sangivamycin for 48 h and subjected to immunocytochemical analysis. Active form of dually phosphorylated JNK (*red*) was detected only in cells where PKCδ (*green*) was observed (indicated with yellow arrowheads). Small white color arrows indicate cells expressing PKCδ siRNA, in which neither phosphorylated JNK nor PKCδ was observed.

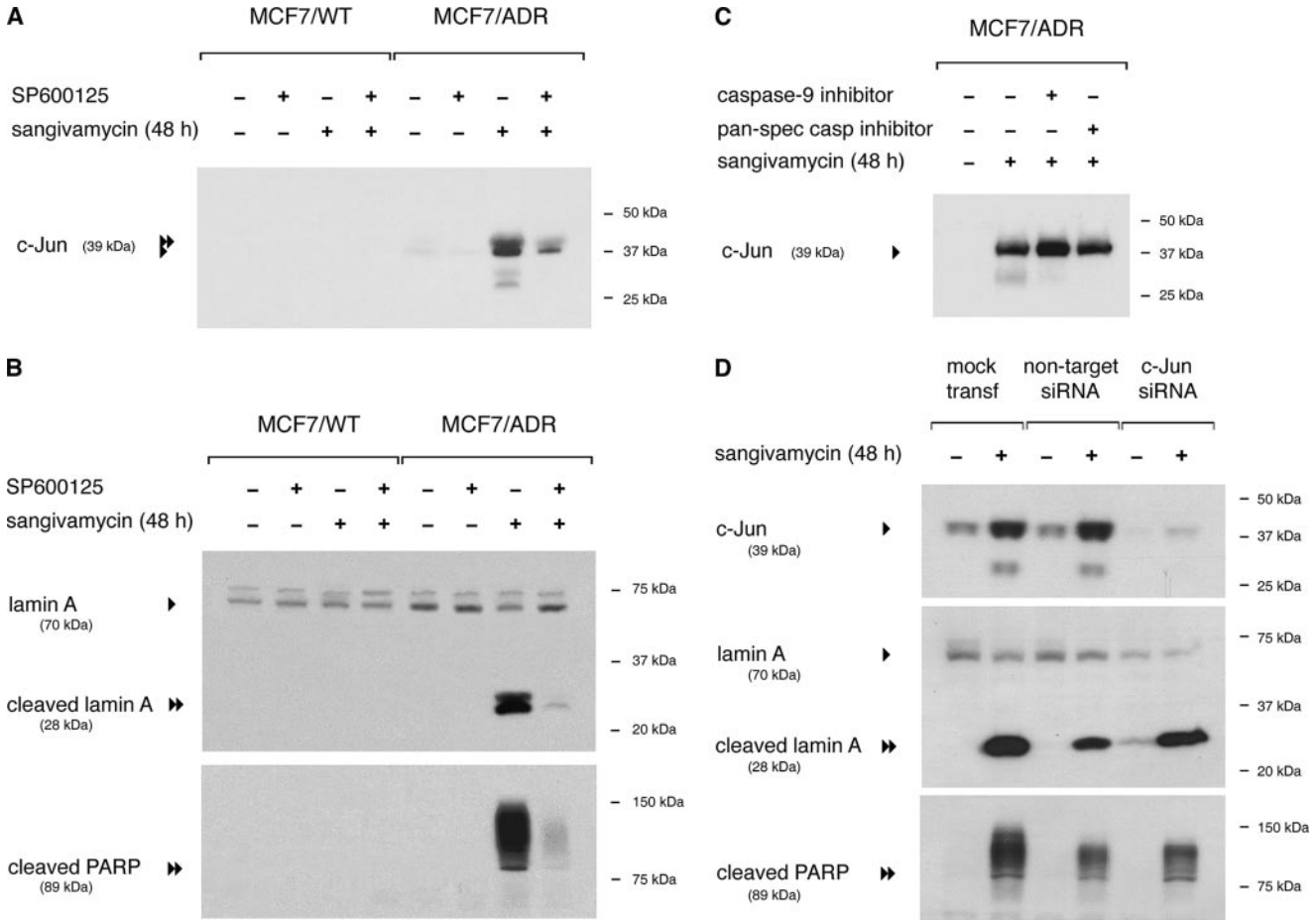

FIGURE 6. **Abolition of sangivamycin-induced caspase-9 activity by inhibition of JNK in MCF7/ADR cells.** Cells were pretreated with 20 μM SP600125 for 1 h before treatment with 0.3 μM sangivamycin for 48 h and subjected to immunoblot analysis. *A*, inhibition of sangivamycin-induced JNK activity in MCF7/ADR cells by pretreatment with SP600125. The *single arrowhead* indicates the nonphosphorylated form of c-Jun, and the *double arrowhead* indicates the presumably phosphorylated form of c-Jun. *B*, inhibition of sangivamycin-induced cleavage of lamin A and PARP in MCF7/ADR cells by pretreatment with SP600125. Cleavage of lamin A and PARP was analyzed using antibodies specific for the full-length and the 28-kDa fragment of lamin A and for the 89-kDa cleaved fragment of PARP. *C*, sangivamycin-induced activation of JNK is upstream of caspase-9 activation in MCF7/ADR cells. MCF7/ADR cells were pretreated with 25 μM caspase-9 inhibitor or 50 μM pan-specific caspase inhibitor for 1 h before treatment of cells with 0.3 μM sangivamycin for 48 h. Immunoreactivity to c-Jun was determined using an antibody recognizing both nonphosphorylated and phosphorylated form of c-Jun. *D*, sangivamycin-induced cleavage of lamin A and PARP in c-Jun siRNA-expressing MCF7/ADR cells. MCF7/ADR cells were transfected with c-Jun siRNA or non-targeting pool siRNA as a negative control. At 48 h after transfection, cells were treated with 0.3 μM sangivamycin for an additional 48 h. The accumulation of c-Jun protein and cleavage products of lamin A and PARP were subsequently determined by immunoblot analysis.

induction was examined in MCF7 cells pretreated with SP600125, a specific inhibitor of JNK activity, before exposure to sangivamycin (Fig. 6*A*). Pretreatment of MCF7/ADR cells with 20 μM SP600125 markedly reduced the induction of both phosphorylated form of c-Jun (upper band of c-Jun doublet) and nonphosphorylated form of c-Jun (lower band) after sangivamycin treatment. Reduction in the accumulation of total c-Jun is ascribed to the positive feedback regulation of c-Jun transcription. SP600125 alone did not affect c-Jun induction in either MCF7/ADR cells or MCF7/WT cells. Sangivamycin-induced cleavage of lamin A and PARP in MCF7/ADR cells was also significantly reduced when cells were pretreated with SP600125 (Fig. 6*B*), suggesting that the caspase cascade activation observed in MCF7/ADR cells treated with sangivamycin (Fig. 4*B*) is downstream of JNK activation. Although pretreatment of MCF7/ADR cells with caspase-9 inhibitor or pan-specific caspase inhibitor abolished sangivamycin-induced cleavage of lamin A and PARP (Fig. 4*C*), such treatment did not reduce sangivamycin-induced c-Jun expression (Fig. 6*C*), which further confirms the notion that activation of caspases is downstream of JNK activation. Increased c-Jun activity has been linked to two apparently opposing physiological consequences, triggering either cell proliferation or apoptosis (61).

To investigate whether the marked induction of c-Jun in sangivamycin-treated MCF7/ADR cells is a prerequisite for the sangivamycin-induced apoptosis in these cells, a c-Jun siRNA expression vector was transiently transfected into MCF7/ADR cells, and sangivamycin-induced cleavage of lamin A and PARP was subsequently examined (Fig. 6*D*). Transfection of MCF7/ADR cells with c-Jun siRNA almost abolished basal expression and greatly reduced induction of c-Jun by sangivamycin, whereas the control transfection with non-target siRNA did not affect either basal expression or induction of c-Jun. However, sangivamycin-induced cleavage of lamin A and PARP was not reduced in MCF7/ADR cells expressing c-Jun siRNA when compared with that in non-target siRNA-expressing cells. These data suggest that the marked induction of c-Jun observed in sangivamycin-treated MCF7/ADR cells is a cellular response

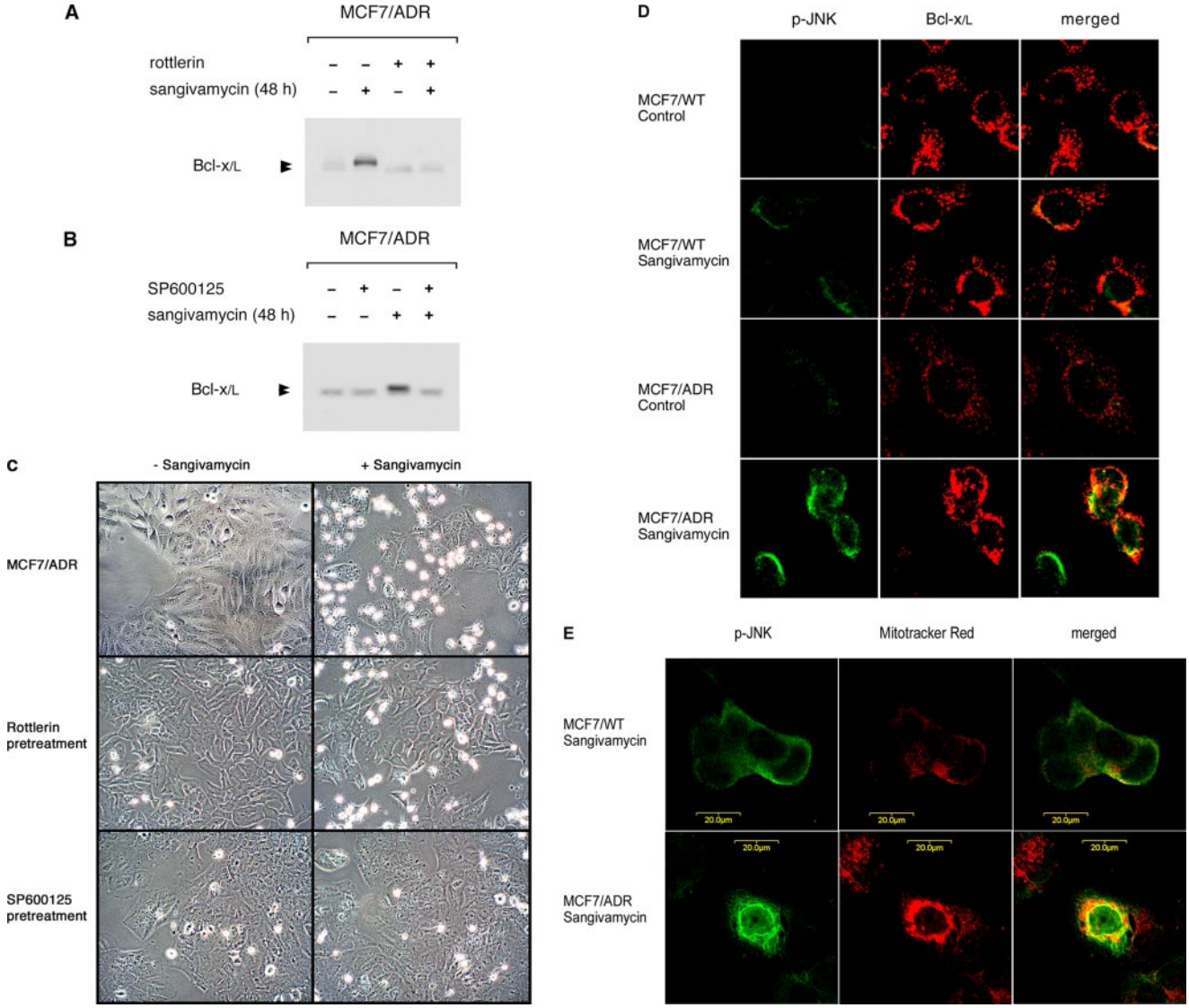

FIGURE 7. **PKCδ- and JNK-dependent phosphorylation of Bcl-x/L in sangivamycin-treated MCF7/ADR cells.** Cells were pretreated with 20 μM rottlerin (*A*) or 20 μM SP600125 (*B*) for 1 h before treatment of cells with 0.3 μM sangivamycin for 48 h. The *double arrowhead* indicates Bcl-x/L doublet bands consisting of phosphorylated and nonphosphorylated Bcl-x/L bands. *C*, inhibitory effects of rottlerin and SP600125 on sangivamycin-induced apoptosis in MCF7/ADR cells. Chemosensitivity to sangivamycin with or without pretreatment with rottlerin or SP600125 was visually evaluated by using an Olympus Vanox microscopy. *D*, co-localization of Bcl-x/L and active form of dually phosphorylated JNK in sangivamycin-treated MCF7/ADR cells. Immunofluorescence of Bcl-x/L (*red*) and phosphorylated JNK (*p-JNK*) (*green*) was detected using an Olympus Fluoview FV300 confocal laser microscope system. *E*, co-localization of active form of dually p-JNK and Mitotracker Red in sangivamycin-treated MCF7/ADR cells. After treatment of cells with 0.3 μM sangivamycin for 48 h, cells were stained with Mitotracker Red, a mitochondrion-selective cell permeant fluorescent stain, and subsequently subjected to immunocytochemical analysis. Immunofluorescence of phosphorylated JNK was detected by confocal microscopy. Co-localization of phosphorylated JNK (*green*) and Mitotracker Red (*red*) in sangivamycin-treated MCF7/ADR cells is represented as *yellow color* immunofluorescence.

to the sangivamycin-induced JNK activation but is dispensable for sangivamycin-induced apoptosis in these cells.

Protein Kinase Cδ and JNK-dependent Phosphorylation of Bcl-x/L in Sangivamycin-treated MCF7/ADR Cells—JNK-mediated phosphorylation of Bcl-x/L has been shown to render various cancer cells more susceptible to apoptotic cell death by inactivating the normal anti-apoptotic activity of Bcl-x/L (71–75). Phosphorylation of Bcl-x/L can be detected as more slowly migrating bands on Western blot (71–73). Treatment of MCF7/ADR cells with sangivamycin resulted in the induction of the slower migrating, presumably phosphorylated form of Bcl-x/L, and this induction was significantly inhibited when cells were pretreated with rottlerin, a specific inhibitor of PKCδ (Fig. 7*A*), or SP600125, a specific inhibitor of JNK (Fig. 7*B*). Under the same experimental conditions, pretreatment of MCF7/ADR cells with these inhibitors significantly block the production of apoptotic cells (Fig. 7*C*), strongly suggesting that activation of PKCδ and JNK are involved in the process of sangivamycin-induced apoptosis.

To determine if the activated form (dually phosphorylated on threonine and tyrosine residues) of JNK was co-localized with mitochondrial protein Bcl-x/L, confocal immunofluorescence microscopic analysis was performed (Fig. 7*D*). As expected, no active form of JNK was detectable in both untreated MCF7/ADR and MCF7/WT cells. After sangivamycin treatment, a significantly enhanced JNK activity was observed in MCF7/ADR cells, whereas a barely detectable level of JNK activity was observed in MCF7/WT cells. Consistent with the data shown in

Fig. 3, Bcl-x/L was abundant in MCF7/WT and was not changed significantly after sangivamycin treatment. In contrast, a lower basal level of Bcl-x/L was detected in MCF7/ADR cells, which was induced significantly after sangivamycin treatment. Moreover, the co-localization of phosphorylated JNK and Bcl-x/L was apparent only in sangivamycin-treated MCF7/ADR cells. Mitochondrial localization of the active form of dually phosphorylated JNK was further confirmed by using Mitotracker Red, a mitochondrion-selective cell-permeant fluorescent stain (Fig. 7*E*). The significant amount of Mitotracker Red was co-localized with the phosphorylated JNK present in sangivamycin-treated MCF7/ADR cells, whereas the co-localization in sangivamycin-treated MCF7/WT cells was hardly detectable. These data strongly suggest that sangivamycin-induced apoptosis in MCF7/ADR cells is mediated at least in part via phosphorylation of the mitochondrial protein Bcl-x/L in a manner that requires the sequential activation of PKCδ and JNK.

DISCUSSION

Our data demonstrate that sangivamycin exerts differential cytotoxic effects in drug-sensitive MCF7/WT and multidrug-resistant MCF7/ADR human breast carcinoma cells. Based on morphological observations, fluorescence-activated cell sorter analysis, and biochemical analysis of apoptotic marker proteins, submicromolar concentrations of sangivamycin induce significant apoptotic cell death in MCF7/ADR cells and significant growth arrest without detectable apoptosis in the parental MCF7/WT cells. Sangivamycin also induces early cell cycle arrest at the G_2/M phase (within 24 h) in both MCF7/WT and MCF7/ADR cells and late arrest at G_1 phase (by 48 h) in MCF7/WT cells but not in MCF7/ADR cells. The apoptotic death of MCF7/ADR cells occurs in the G_2/M-arrested subpopulation.

Further characterization of various biochemical events accompanying growth arrest and apoptosis in these two cell lines demonstrate striking differences in the relative amounts of several proteins. First, treatment of MCF7/WT cells with sangivamycin results in increased p53 accumulation followed by increased accumulation of $p21^{Waf1/Cip1}$ after a 24-h lag period, consistent with a p53-dependent induction of $p21^{Waf1/Cip1}$ expression. Therefore, the sustained activation and induction of p53 and p21 as well as the persistent G_2 cell cycle arrest observed in MCF7/WT cells might account, at least in part, for the sangivamycin-induced prolonged growth arrest. In this view, both the irreversible G_2 cell cycle arrest and the subsequent apoptotic death of MCF7/ADR cells could be ascribed, at least in part, to an inactive p53 and non-detectable level of p21. Interestingly, our MCF7/WT data demonstrate a significant sangivamycin-induced accumulation of 40–50-kDa proteins that have cross-immunoreactivity to the p53 antibody, consistent with recent reports showing proteolytic cleavage products of p53 (into 50-, 40-, and 35-kDa fragments) via its interaction with damaged DNA *in vitro* (77–79). Although sangivamycin promotes apparently similar p53 proteolytic cleavage, it does not induce a significant amount of DNA damage in MCF7/WT cells as assessed by monitoring the formation of foci of either phospho-p53 (serine 15) or a widely-used surrogate marker for DNA damage response, γ-H2AX, although such foci formation was detected in sangivamycin-treated MCF7/ADR cells (supplemental Fig. 2*A*). DNA damage-induced foci were apparent in both cell lines after irradiation (supplemental Fig. 2*B*). Although further investigation is needed, we tentatively conclude that the presumed proteolytic p53 products produced in sangivamycin-treated MCF7/WT cells are not generated by DNA damage.

Second, relative amounts of pro- and anti-apoptotic proteins (at least four Bcl-2-related proteins) present in these two cell lines are very different. MCF7/WT cells contain relatively higher level of two anti-apoptotic proteins, Bcl-2 and Bcl-x/L, whereas MCF7/ADR cells contain the relatively higher level of a proapoptotic protein, Bcl-x/S. Furthermore, sangivamycin induces a persistent activation and translocation of JNK to mitochondria in MCF7/ADR cells, presumably phosphorylating Bcl-x/L in mitochondria, consistent with the recent findings that dimerization and post-translational modifications such as phosphorylation can alter the function of these proteins (72–76). Although a role for c-Jun in apoptosis has been demonstrated (61), our data with c-Jun siRNA indicate that the marked induction of c-Jun activity is dispensable for the sangivamycin-induced apoptosis of MCF7/ADR cells.

Stepwise analyses of our findings with PKCδ siRNA and various pharmacological inhibitors (rottlerin, SP600125, caspase-9 inhibitor, and pan-specific caspase inhibitor) support that sangivamycin-induced apoptosis in MCF7/ADR cells is mediated through the sequential activation of PKCδ, JNK, the mitochondrial apoptotic pathway acting via phosphorylation of Bcl-x/L, and then activation of the caspase-9 cascade, leading to the activation of caspase-6 and -7 and subsequent cleavage of lamin A and PARP. Taken together, the sangivamycin-induced apoptotic pathway is supported by the observations that (i) sangivamycin induces persistent phosphorylation of c-Jun on serine 63 and 73 and a marked induction of c-Jun expression in MCF7/ADR cells but not in MCF7/WT cells, (ii) sangivamycin induces phosphorylation of Bcl-x/L in MCF-7/ADR cells, (iii) sangivamycin induces cleavage of procaspase-9, -6, and -7 to active caspases in MCF7/ADR cells but not in MCF7/WT cells, (iv) sangivamycin induces cleavage of death-substrates lamin A and PARP in MCF7/ADR cells but not in MCF7/WT cells, (v) preincubation of cells with a specific JNK inhibitor, SP600125, abolishes sangivamycin-induced c-Jun phosphorylation and induction, Bcl-x/L phosphorylation, and cleavage of lamin A and PARP, (vi) preincubation with caspase-9 inhibitor significantly suppresses sangivamycin-induced cleavage of lamin A and PARP but not phosphorylation and expression of c-Jun, (vii) preincubation with the PKCδ inhibitor, rottlerin, abolishes sangivamycin-induced c-Jun phosphorylation and expression, Bcl-x/L phosphorylation, caspase-9 activation, and cleavage of lamin A and PARP, and (viii) suppression of PKCδ expression or activity by siRNA or anti-PKCδ, respectively, abolishes activation of JNK. These results suggest that the sangivamycin-induced apoptosis of MCF7/ADR cells requires the induction of PKCδ activity as an upstream signal transducer.

In conclusion, our data indicate that sangivamycin can exert chemotherapeutic activity by manipulating at least two key processes, cell cycle arrest and apoptosis. Depending upon the array or balance of cellular signal transducing proteins

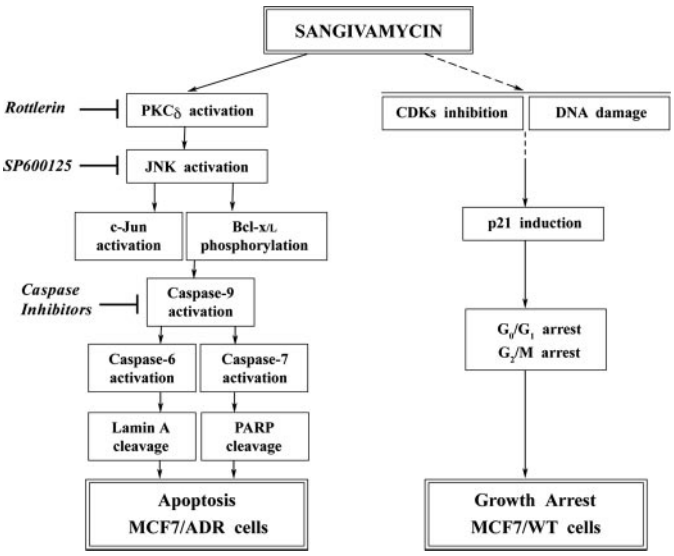

FIGURE 8. **Modes of action of sangivamycin.** Proposed models for how sangivamycin affects various biochemical processes and events in MCF7/WT and MCF7/ADR cells leading to the differential cytotoxic effects in these cell lines are illustrated in this schematic diagram. *CDK*, cyclin-dependent kinase.

expressed in untreated cells, sangivamycin exposure triggers different signal transduction pathways, leading to different outcomes, apoptosis or growth arrest. Whether an apoptotic response will always occur in various multidrug-resistant breast cancer cells treated with sangivamycin whereas isogenic drug sensitive cells will respond with only growth arrest remains to be determined. Under our experimental conditions, sangivamycin-induced apoptosis in MCF7/ADR multidrug-resistant breast cancer cells is characterized by an irreversible G_2/M cell cycle arrest, the sequential activation of PKCδ, JNK, and caspase-9, which is led to a massive apoptotic cell death. The molecular mechanism underlying G_2/M cell cycle arrest remains unknown. The proposed working models (Fig. 8) for the molecular basis of two different sangivamycin-induced effects at the cellular level can be tested in multiple ways, which if confirmed would provide invaluable insights for approaches to the development of effective chemotherapy by targeting appropriate signal transducer that may, however, vary in different type of cancers.

Acknowledgments—We thank Drs. Wayne B. Anderson at NCI, National Institutes of Health and Thomas Mattson at Georgetown University for scientific discussions and Dr. Kenneth Cowan for providing MCF7/WT cells and MCF7/ADR cells.

REFERENCES

1. Bergstrom, D. E., Brattesani, A. J., Ogawa, M. K., Reddy, P. A., Schweickert, M. J., Balzarini, J., and De Clercq, E. (1984) *J. Med. Chem.* **27,** 285–292
2. Turk, S. R., Shipman, C., Jr., Nassiri, R., Genzlinger, G., Krawczyk, S. H., Townsend, L. B., and Drach, J. C. (1987) *Antimicrob. Agents Chemother.* **31,** 544–550
3. Ritch, P. S., Glazer, R. I., Cunningham, R. E., and Shackney, S. E. (1981) *Cancer Res.* **41,** 1784–1788
4. Glazer, R. I., Hartman, K. D., and Cohen, O. J. (1981) *Biochem. Pharmacol.* **30,** 2697–2701
5. Cohen, M. B., and Glazer, R. I. (1985) *Mol. Pharmacol.* **27,** 349–355
6. Cavins, J. A., Hall, T. C., Olson, K. B., Khung, C. L., Horton, J., Colsky, J., and Shadduck, R. K. (1967) *Cancer Chemother. Rep.* **51,** 197–200
7. Hardesty, C. T., Chaney, N. A., Waravdekar, V. S., and Mead, J. A. (1974) *Cancer Res.* **34,** 1005–1009
8. Robins, R. K., and Revankar, G. R. (1985) *Med. Res. Rev.* **5,** 273–296
9. Migawa, M. T., Drach, J. C., and Townsend, L. B. (2005) *J. Med. Chem.* **48,** 3840–3851
10. Ding, Y., An, H., Hong, Z., and Girardet, J. L. (2005) *Bioorg. Med. Chem. Lett.* **15,** 725–727
11. Ravelo, A. G., Estevez-Braun, A., Chavez-Orellana, H., Perez-Sacau, E., and Mesa-Siverio, D. (2004) *Curr. Top. Med. Chem.* **4,** 241–265
12. Biron, K. K., Harvey, R. J., Chamberlain, S. C., Good, S. S., Smith, A. A., III, Davis, M. G., Talarico, C. L., Miller, W. H., Ferris, R., Dornsife, R. E., Stanat, S. C., Drach, J. C., Townsend, L. B., and Koszalka, G. W. (2002) *Antimicrob. Agents Chemother.* **46,** 2365–2372
13. Koszalka, G. W., Good, S. S., Boyd, L., Drach, J. C., Townsend, L. B., and Biron, K. K. (2002) *Antimicrob. Agents Chemother.* **46,** 2373–2380
14. Loomis, C. R., and Bell, R. (1988) *J. Biol. Chem.* **263,** 1682–1692
15. Osada, H., Sonoda, T., Tsunoda, K., and Isono, K. (1989) *J. Antibiot. (Tokyo)* **42,** 102–106
16. Palczewski, K., Kahn, N., and Hargrave, P. A. (1990) *Biochemistry* **29,** 6276–6282
17. Saffer, J. D., and Glazer, R. L. (1981) *Mol. Pharmacol.* **20,** 211–217
18. Osada, H., Cui, C.-B., Onose, R., and Hanaoka, F. (1997) *Bioorg. Med. Chem.* **5,** 193–203
19. Kim, M. K., Cho, Y.-H., Kim, J. M., Chun, M. W., Lee, S. K., Lim, Y., and Lee, C.-H. (2005) *Cancer Lett.* **223,** 239–247
20. Tobiume, K., Matsuzawa, A., Takahashi, T., Nishitoh, H., Morita, K., Takeda, K., Minowa, O., Miyazono, K., Noda, T., and Ichijo, H. (2001) *EMBO Rep.* **2,** 222–228
21. Hengartner, M. O. (2000) *Nature* **407,** 770–776
22. Thompson, C. B. (1995) *Science* **267,** 1456–1462
23. Los, M., Wesselborg, S., and Schuize-Osthoff, K. (1999) *Free Immunity* **10,** 629–639
24. Yuan, J., and Yankner, B. A. (2000) *Nature* **407,** 802–809
25. Rao, L., and White, E. (1997) *Curr. Opin. Genet. Dev.* **7,** 52–58
26. Kroemer, G. (1997) *Nat. Med.* **3,** 614–620
27. Nuñez, G., Benedict, M. A., Hu, Y., and Inohara, N. (1998) *Oncogene* **17,** 3237–3245
28. Gross, A., McDonnell, J. M., and Korsmeyer, S. J. (1999) *Genes Dev.* **13,** 1899–1911
29. Oltvai, Z. N., Milliman, C. L., and Korsmeyer, S. J. (1993) *Cell* **74,** 609–619
30. Wei, M. C., Zong, W. X., Cheng, E. H., Lindsten, T., Panoutsakopoulou, V., Ross, A. J., Roth, K. A., MacGregor, G. R., Thompson, C. B., and Korsmeyer, S. J. (2001) *Science* **292,** 727–730
31. Leszczynski, D. (1995) *Oncol. Res.* **7,** 471–480
32. Lucas, M., and Sanchez-Margalet, V. (1995) *Gen. Pharmacol.* **26,** 881–887
33. Reyland, M. E., Anderson, S. M., Matassa, A. A., Barzen, K. A., and Quissell, D. O. (1999) *J. Biol. Chem.* **274,** 19115–19123
34. DalPra, I., Whitfield, J. F., Chiarini, A., and Armato, U. (2000) *Exp. Cell Res.* **255,** 171–183
35. Goubout, J. P., Pesavento, J., Hartman, M. E., Manson, S. R., and Freund, G. G. (2002) *J. Biol. Chem.* **277,** 2554–2561
36. Emoto, Y., Kisaki, H., Manome, Y., Kharbanda, S., and Kufe, D. (1996) *Blood* **87,** 1991–1996
37. Mizuno, K., Noda, K., Araki, T., Imaoka, T., Kobayashi, Y., Akita, Y., Shimonaka, M., Kishi, S., and Ohno, S. (1997) *Eur. J. Biochem.* **250,** 7–18
38. Frasch, S. C., Henson, P. M., Kailey, J. M., Richter, D. A., Janes, M. S., Fadok, V. A., and Bratton, D. L. (2000) *J. Biol. Chem.* **275,** 23065–23073
39. Kharbanda, S., Pandey, P., Ren, R., Mayer, B., Zon, L., and Kufe, D. (1995) *J. Biol. Chem.* **270,** 30278–30281
40. Verheij, M., Bose, R., Lin, X. H., Yao, B., Jarvis, W. D., Grant, S., Birrer, M. J., Szabo, E., Zon, L. I., Kyriakis, J. M., Haimovitz-Friedman, A., Fuks, Z., and Kolesnick, R. N. (1996) *Nature* **380,** 75–79
41. Testolin, L., Carson, C., Wang, Y., Walker, P. R., Armato, U., and Sikorska, M. (1997) *Exp. Cell Res.* **230,** 220–232
42. Derijard, B., Hibi, M., Wu, I. H., Barrett, T., Su, B., Deng, T., Karin, M., and Davis, R. J. (1994) *Cell* **76,** 1025–1037
43. Gupta, S., Campbell, D., Derijard, B., and Davis, R. J. (1995) *Science* **267,**

389–393
44. Yamamoto, K., Ichijo, H., and Korsmeyer, S. J. (1999) *Mol. Cell. Biol.* **19,** 8469–8478
45. Lei, K., and Davis, R. J. (2003) *Proc. Natl. Acad. Sci. U. S. A.* **100,** 2432–2437
46. Lee, S. A., Karaszkiewicz, J. W., and Anderson, W. B. (1992) *Cancer Res.* **52,** 3750–3759
47. Lee, S. A., Dritschilo, A., and Jung, M. (2001) *J. Biol. Chem.* **276,** 11783–11790
48. Bradford, M. M. (1976) *Anal. Biochem.* **72,** 248–254
49. Bunz, F., Dutriaux, A., Lengauer, C., Waldman, T., Zhou, S., Brown, J. P., Sedivy, J. M., Kinzler, K. W., and Vogelstein, B. (1998) *Science* **282,** 1497–1501
50. Amellem, O., Stokke, T., Sandvik, J. A., Smedshammer, L., and Pettersen, E. O. (1990) *Exp. Cell Res.* **232,** 361–370
51. Ogretmen, B., and Safa, A. R. (1997) *Oncogene* **14,** 499–506
52. Cai, Z., Capoulade, C., Moyret-Lalle, C., Amor-Gueret, M., Feunteun, J., Larsen, A. K., Paillerets, B. B., and Chouaib, S. (1997) *Oncogene* **15,** 2817–2826
53. Orth, K., Chinnaiyan, A. M., Garg, M., Froelich, C. J., and Dixit, V. M. (1996) *J. Biol. Chem.* **271,** 16443–16446
54. Duan, H., Chinnaiyan, A. M., Hudson, P. L., Wing, J. P., He, W. W., and Dixit, V. M. (1996) *J. Biol. Chem.* **271,** 1621–1625
55. Cohen, G. M. (1997) *Biochem. J.* **326,** 1–16
56. Goldberg, M., Harel, A., and Gruenbaum, Y. (1999) *Crit. Rev. Eukaryot. Gene Expression* **9,** 285–293
57. Oberhammer, F. A., Hochegger, K., Froschl, G., Tiefenbacher, R., and Pavelka, M. (1994) *J. Cell Biol.* **126,** 827–837
58. Rao, L., Perez, D., and White, E. (1996) *J. Cell Biol.* **135,** 1441–1455
59. Virag, L., and Szabo, C. (2002) *Pharmacol. Rev.* **54,** 375–429
60. Oliver, F. J., de la Rubia, G., Rolli, V., Ruiz-Ruiz, M. C., de Murcia, G., and Murcia, J. M. (1998) *J. Biol. Chem.* **273,** 33533–33539
61. Bossy-Wetzel, E., Bakiri, L., and Yaniv, M. (1997) *EMBO J.* **16,** 1695–1709
62. Smeal, T., Hibi, M., and Karin, M. (1994) *EMBO J.* **13,** 6006–6010
63. Binetruy, B., Smeal, T., and Karin, M. (1991) *Nature* **351,** 122–127
64. Devary, Y., Gottlieb, R. A., Smeal, T., and Karin, M. (1992) *Cell* **71,** 1081–1091
65. Radler-Pohl, A., Sachsenmaier, C., Gebel, S., Auer, H. P., Bruder, J. T., Rapp, U., Angel, P., Rahmsdorf, H. J., and Herrlich, P. (1993) *EMBO J.* **12,** 1005–1012
66. Smeal, T., Binetruy, B., Mercola, D. A., Birrer, M., and Karin, M. (1991) *Nature* **354,** 494–496
67. Lei, K., Nimnual, A., Zong, W. X., Kennedy, N. J., flavell, R. A., Thompson, C. B., Bar-Sagi, D., and Davis, R. J. (2002) *Mol. Cell. Biol.* **22,** 4929–4942
68. Palmada, M., Kanwal, S., Rutkoshi, N. J., Gustafson-Brown, C., Johnson, R. S., Wisdom, R., and Carter, B. D. (2002) *J. Cell Biol.* **158,** 453–461
69. Tournier, C., Hess, P., Yang, D. D., Xu, J., Turner, T. K., Nimnual, A., Bar-Sagi, D., Jones, S. N., Flavell, R. A., and Davis, R. J. (2000) *Science* **288,** 870–874
70. Willis, S., Day, C. L., Hinds, M. G., and Huang, D. C. S. (2003) *J. Cell Sci.* **116,** 4053–4056
71. Yang, D. D., Kuan, C. Y., Whitmarsh, A. J., rincon, M., Zheng, T. S., Davis, R. J., Rakic, P., and Flavell, R. A. (1997) *Nature* **389,** 865–870
72. Basu, A., and Haldar, S. (2003) *FEBS Lett.* **538,** 41–47
73. Fan, M., Goodwin, M., Vu, T., Brantley-Finley, C., Gaarde, W. A., and Chambers, T. C. (2000) *J. Biol. Chem.* **275,** 29980–29985
74. Drew, L., Fine, R. L., Do, T. N., Douglas, G. P., and Petrylak, D. P. (2002) *Clin. Cancer Res.* **8,** 3922–3932
75. Schroeter, H., Boyd, C. S., Ahmed, R., Spencer, J. P. E., Duncan, R. F., Rice-Evans, C., and Cadenas, E. (2003) *Biochem. J.* **372,** 359–369
76. Kharbanda, S., Saxena, S., Yoshida, K., Pandey, P., Kaneki, M., Wang, Q., Cheng, K., Chen, Y., Campbell, A., Sudha, T., Yuan, Z., Narula, J., Weichselbaum, R., Nalin, C., and Kufe, D. (2000) *J. Biol. Chem.* **275,** 322–327
77. Okorokov, A. L., and Milner, J. (1997) *Oncol. Res.* **9,** 267–273
78. Gelis, C., Mavon, A., and Vicendo, P. (2005) *Photochem. Photobiol.* **81,** 975–982
79. Molinari, M., Okorokov, A. L., and Milner, J. (1996) *Oncogene* **13,** 2077–2086